объединенный
институт
ядерных
исследований
дубна

E13-94-97

P.A.Kulinich

USAGE OF SHAPE OF SIGNAL FROM LIQUID IONIZATION CHAMBER FOR REJECTION DELTA ELECTRONS AND MULTIPLE MEASUREMENT OF *dE/dx*

Submitted to «Nuclear Instruments and Methods»

1994

Кулинич П.А. E13-94-97

Использование формы сигнала с жидкостной ионизационной камеры для режекции дельта-электронов и многократного измерения dE/dx

Предлагается метод и описываются результаты численного моделирования разделения различных заряженных частиц с $\beta < 0.9$ в плоской жидкостной ионизационной камере со временем дрейфа несколько микросекунд. Предлагается использовать форму сигнала с выхода предусилителя, подключенного к ионизационной камере толщиной $L > 2$ см, для исключения ионизационных потерь дельта-электронов с энергией выше или порядка 1 МэВ. Метод анализа формы сигнала позволяет получить несколько значений dE/dx внутри одного зазора однородной ионизационной камеры. Показана возможность разделения π- и k-мезонов на уровне 2σ для диапазона импульсов (0,5—0,8) ГэВ/с в 4-сантиметровой камере с жидким криптоном.

Работа выполнена в Лаборатории ядерных проблем ОИЯИ.

Препринт Объединенного института ядерных исследований. Дубна, 1994

Kulinich P.A. E13-94-97

Usage of Shape of Signal from Liquid Ionization Chamber for Rejection Delta Electrons and Multiple Measurement of dE/dx

The results of numerucal simulation of separation of different kinds of charged particles with $\beta < 0.9$ in the uniform ionization liquid medium chamber with a drift time of few microseconds is described. A waveform of the preamplifier output signal connected to a thick gap ($L > 2$ cm) ionization liquid medium chamber is proposed to be used for rejection of energetic delta electrons and for few measurements of dE/dx inside one gap. Possibility of separating π- and k-mesons at the level of 2σ in a 4 cm LKr medium chamber in the momentum range (0.5 N $\div$ 0.8) GeV/c is shown.

The investigation has been performed at the Laboratory of Nuclear Problems, JINR.

Preprint of the Joint Institute for Nuclear Research. Dubna, 1994

1. Introduction

Use of liquid medium ionization detectors is attractive due to the possibility of obtaining good energy and spatial resolution. That is why they are widely used in the field of elementary particles or astrophysics experiment [1]. Often, such a detector consists of a set of parallel ionizing chambers, which allows multiple released energy information to be used for *dE/dx* analysis [2]. This ability of particle separation can improve the performance of the total setup. For separation one can use the amplitude information from few consecutive layers along the particle track [2,3]. But in the case of thick layers the total thickness of the medium would be large enough to cause significant influence of the nuclear interaction.

Usually the fast electron component pulses from the ionization chamber are analyzed with a low noise charge sensitive preamplifier followed by a shaper for amplification and shaping. The amplitude of the output signal of the integrating preamplifier is proportional to the total collected charge of free electrons, and it is roughly proportional to the free electrons' charge released in the gap [4] (see Appendix A). But in principle strong proportionality occurs only in the case of uniform primary ionization. Otherwise the shape and amplitude at the output of the preamplifier depend on the ionization distribution in the gap of the chamber. The possibility of analysis of the shape of the preamplifier output signal for extracting few measurements of *dE/dx* from one gap of a liquid medium ionization chamber is discussed below.

1.1 The influence of δ-electrons

For beginning, one have to point out that the problem of particle identification using few values of energy loss rates *dE/dx* for heavy charged projectiles is mainly related to influence of energetic delta-electrons (*δe-*). The additional ionization caused by *δe-* is superimposed on that of primary particle. So the right tail (as in Landau distribution) of the distribution of collected charge for relativistic particles (Fig. 1a) is determined by the rare energetic *δe-*. In order to obtain non-shifted estimation of the most probable *dE/dx* value for the main track one should "reject" the parts of the track inside a gap of the chamber which have significant additional ionization by the *δe-*. The mean value of *dE/dx** at the rest path will have more symmetrical and narrower distribution (Fig. 1b) and therefore permits improving separation of the particles with nearly equal mean values of the energy loss rates.

For the quantitative difference in energy loss rates for two particles at a given momentum the relative difference in energy *RDE*=ABS(*E1*-*E2*)/MIN(*E1*,*E2*) has to be evaluated. Fig. 2a depicts the total and restricted [5] energy loss rates, when ionization by δ-electrons with energy over E_{max} is not taken into account. The corresponding plots of the RDE_{tot} and relative difference of the restricted energy loss rates RDE_{rst} for few values of cutoff energy of δ-electrons (E_{max} =0.1, 2.0 MeV) are shown in Fig. 2b. It is seen that significant part of the mean energy loss rates (about 30%) is produced by δ-electrons, and the relative difference of restricted energy loss rates RDE_{rst} is higher than that for total energy loss rate RDE_{tot} at low momentum. However at higher momentum RDE_{rst} is saturated at lower meaning of the ratio of restricted energy loss rates of two kinds of particles. So, rejection of the δ-electron influence can improve particle separation at low momentum (below minimum of RDE_{rst}) but at higher momentum the separation becomes worse.

2. Review of the study

Ionization yield of penetrating charged particles and secondary energetic δ-electrons in medium of the chamber were simulated. After that information about space distribution of ionization density and simulated electronic noise was used to calculate the shape of the signal at the output of the integrating preamplifier. Then the output signal was "digitized" by Fast Analog to Digit Converter (FADC), and the "second derivative" of signal gave, finally, *dE/dx* information per few layers inside a gap of the ionization chamber. This approach permits one to find an algorithm of rejections of the energetic *δe-* influence.

2.1 Assumption

It is assumed that all tracks of the particles are orthogonal to the chamber plane, and its distance to the edge of electrode (and consequently the dimensions of the electrode) are supposed to be mach more than the thickness of the gap of the chamber. Otherwise the shape of the current signal from a pad is a complicated function of the track position.

In this study the intensity of the recombination process of the ionization on the primary particle track and on the path of arising δ-electrons is assumed to be equal. It is known [6] that the charge response measured with the ^{207}Bi source in a parallel plate chamber depends significantly on the level of impurities. It can be less than 50% of the charge collected in pure krypton. In calculation of collected charge the *w*-value of liquid krypton was used to obtain the number of primary ionized pairs, then it was divided by fixed factor K_w to calculate the number of free electrons available after recombination.

The code is able to take into account the simple exponential model of free electron life time, but the following results were obtained for the large value of life time to drift time ratio. Similarly, transition time of preamplifier should be much smaller than the drift time. The liberated energetic $\delta e-$ with the energy larger than few MeV will travel a macroscopic distance before it is stopped and it produces additional ionization along its path. The angular distribution of $\delta e-$ was calculated according to kinematics of scattering of primary particle from the fixed electron, though, because of multiple scattering the current angle of electron would change later. As a measure of straight-line penetration distance of such $\delta e-$ the electron "practical range" was used [7].

In principle, the drift of the positive ions created in the ionization process should also contribute to the current. The positive ion mobility in liquid rear gases is, however, five orders of magnitude lower than that for electrons [8], with the current being similarly suppressed, and can therefore be neglected.

The density effect in calculation of the restricted energy loss was neglected because it is significant at higher momentum of incident particles. So for π-meson momentum less than 2 GeV/c the decrease in dE/dx is less than 2.8% after taking into account the expression for the density effect [9].

Krypton gas contains a small amount of the radioactive isotope ^{85}Kr with a half-life of 11 yr. It decays by beta decay with an endpoint energy of 670 keV and releases an average energy of 250 keV [10]. An electron that resulted from β-decays of ^{85}Kr was simulated for each event, too.

2.2 Illustration of method

Let us consider the time dependence of the chamber output current and the integrating preamplifier signal on a gap of the uniform ionization chamber for different distribution of primary ionization in an ideal case of large life time of free electrons.

In the case of local ionization cluster, as for a low energy γ-quantum (Fig. 3a,b), the output current (Fig. 3c) is constant for the total drift time. The drift time is proportional to the cluster distance to the anode. The output signal from the integrating preamplifier (Fig. 3d) is a linear function during

drift time and after that slowly decays with the constant time $\tau=RC$ of preamplifier feed back.

For uniformly spread primary ionization (Fig.4a, 4b) the output current (Fig. 4c) has a triangular shape and the corresponding signal at the preamplifier output (Fig. 4d) has a parabola-like shape.

The superposition of uniformly spread primary ionization and, for example, of two local clusters (Fig. 5a,b) is illustrated in Fig. 5c,d. The main feature of this sample is presence of the "steps" in the current plot, time durations of which are proportional to the length of clusters along the direction of the electric field. The signal at the output of preamplifier (Fig. 5d) will differ from the parabola shape in this case.

This illustration permits one to find the way how one can recognize significant additional ionization determined by energetic delta-electrons. In conclusion, if we have the ideal integrating preamplifier (without noise) then the second derivative of its output signal gives us the dE/dx distribution inside the gap of a uniform ionization chamber.

As was mentioned before, the distance of the track to the edge of the signal electrode (pad) of the chamber (Fig. 6a) should be large enough not to distort significantly the shape of current (Fig. 6b) and corresponding dE/dx (Fig. 6c). For example, for an infinite chamber with a gap of L=2 cm and a signal pad 8*8 cm^2 in size the area with distortion of dE/dx less than 3.6% (7.7%) has the size about 2*2 cm^2 (3*3 cm^2) at the centre of the pad.

2.3 General description of the Monte Carlo simulation

The program code which simulates ionization corresponding to the restricted energy loss of a heavy projectile and produced energetic knock-on electrons was designed. It takes into account the "electronic noise" of the preamplifier, too. In numerical simulation a gap of a uniform ionization chamber L was divided into a large number N_s of thin layers ($dL=L/N_s$), and ionization yield in each layer with thickness dL was calculated as a sum of the constant term (restricted energy loss) and the statistically variable energy loss of delta-electrons.

The restricted energy loss rate (Fig. 2a) of a heavy projectile via all collisions which have energy transfer T such that $T \le E_{max} \ll T_{max}$ was calculated according to the formula [5]:

$$\left(\frac{dE}{dx}\right)_{\le E_{max}} = \frac{1}{2} D \frac{Z_{med}\,\rho_{med}}{A_{med}} \left(\frac{Z_{inc}}{\beta}\right)^2 \left[\ln\left(\frac{E_{max} T_{max}}{I^2}\right) - \beta^2 - \delta - \frac{2C}{Z_{med}} \right]$$

where δ represents the density effect, it is non-negligible only for highly relativistic projectiles in denser media; and C is the correction for low speed projectiles. For a relativistic spinless charged particle the production of high energy δ-electrons of kinetic energy T is given with good approximation by the formula [11]:

$$\frac{d^2N}{dTdx} = \frac{1}{2} D \left(\frac{Z_{med}}{A_{med}}\right) \left(\frac{Z_{inc}}{\beta}\right)^2 \rho_{med} \frac{F}{T^2} ;$$

for $I \ll T \le T_{max}$, where the maximum energy of $\delta e-$ is

$$T_{max} = \frac{2\, m_e \beta^2 \gamma^2 c^2}{1 + 2\gamma \frac{m_e}{M_{inc}} + \left(\frac{m_e}{M_{inc}}\right)^2}$$

$$F = 1 - \frac{T}{T_{max}}$$ for a particle with spin = 0

Here M_{inc} and Z_{inc} are the mass and charge number of the projectile; Z_{med}, A_{med} and ρ_{med} are the charge number, mass number and density of the medium. D=0.307 MeV cm^2 g^{-1}, m_e is the mass of the electron and $I \cong 16\,(Z_{med})^{0.9}$ eV .

The practical range of δ-e was calculated according to the formula [7]: $R_p = AT[1-B/(1+CT)]$ with A=0.55 g cm^{-2}MeV^{-1}, B=0.9841 and C=3.0 MeV^{-1}, where T MeV is the kinematic energy of δe-.

As an illustration, Table 1 shows the values of the calculated mean rate energy loss, maximal energy and density of δ-electrons (dN/dx) and their practical range (R_p) in LKr medium for two kinds of projectiles. It is essential that the higher the

energy of δe-, the smaller the angle of δe- to the primary track.

Table 1. Energy loss of π- and k- mesons and characteristics of arising δe-

	P GeV/c	dE/dx_{tot} MeV/cm	T_{max} MeV	$T_{\delta e-}$ MeV	dN/dx 1/cm	R_p mm
π	0.5	3.44	12.77	> 10 > 7 > 4 > 1	6.8E-4 3.6E-3 1.5E-2 13.E-2	> 22. > 15. > 8.3 > 1.7
k	0.5	4.85	1.04	> 1	9.3E-3	> 1.7
π	0.8	3.59	32.21	> 10 > 7 > 4 > 1	5.6E-3 1.1E-2 2.6E-2 15.E-2	> 22. > 15. > 8.3 > 1.7
k	0.8	3.76	2.67	> 2 > 1	1.1E-2 8.0E-2	> 3.9 > 1.7

For simulation of the preamplifier noise the following approach was used. The noise property of a real preamplifier was estimated in few frequency bands chosen according to the collecting time of the free electrons in the chamber with a 2 cm gap. Then the software generator was designed in order to obtain the same noise to signal ratio in the corresponding frequency bands. Unfortunately an available shaper had the maximal shaping time of 4 μs, so in lower frequency range the noise property of the preamplifier was not measured and the property of the software noise generator was not checked.

The current signal for the model of the preamplifier was calculated according to the mean energy loss of the minimum ionizing particle (MIP) in the 2 cm gap of the LKr chamber. Then its value and drift time T_{dr} were used in measurement with a real preamplifier. The noise influence of the real preamplifier (ENC=550e at τ_{sh}=1μs) was measured with a parabola-like calibration voltage signal at different values of the shaper time constant. The charge, corresponding to the predicted one for MIP, was injected into the preamplifier through a known test capacitor. The signal duration was T_{dr}=6 μs, and the amplitude of the input signal was set at 28 mV. An additional capacitance (C_{in}=82 pF) was attached to the input of the preamplifier during the measurement, thereby keeping the capacitance seen by the preamplifier roughly equal to that during data taking.

A software random noise generator was designed in order to obtain the same noise to signal ratio at the output of the software model of the amplifier-shaper for corresponding shaping time parameters. The preamplifier was modeled as a charge integrating op-amp with a feedback capacitance. A simple *RC-CR* shaper model was used in the calculation.

The following data shows an achieved agreement with the experimentally measured noise level.

Table 2. The relative width of calibration spectra for a real preamplifier test and the result of simulation for different shaping time.

Shaping time	0.25 μs	1.0 μs	2.0 μs	4.0 μs
$FWHM_{exp}$/Mean	3.65%	1.56%	1.06%	0.95%
$FWHM_{sim}$/Mean	3.63%	1.55%	1.11%	0.97%

The code generated π- and *k*- mesons with the same "rate". The signals at the output of the integrating preamplifier has been calculated for the successive set of points with a time pitch dt=20ns. These signals were "digitized" by the model of the real FADC. The set ($N_s=T_{dr}/dt$) of samples during drift time was divided into few groups (N_{gr}=5÷10), and the sum in each group was used for consecutive analysis. As a result of the first subtraction, the set of ($N_{gr}-1$) values of the "current" was available. The second subtraction gave (N_{gr}-2) values of $dE/dx_{mes}(i)$ corresponding to the efficient number of quasi-gaps $N_{qg}=(N_{gr}-2)$.

These values of $dE/dx(i)_{mes}$ are different because of accidental appearance of δ-electrons along the track and because of the preamplifier electronic noise disturbance. Few ways of exclusion of the samples with a large value of $dE/dx(i)_{mes}$ were tested in order to obtain the best separation of two spectra. As a measure of particle separation, the percentage of pions overlapped (POO%) is used hereafter. It is equal to the ratio of the number of the particles in the left (pion) spectrum with deposited energy larger than E_{k15} to total number of particles in this spectrum. The meaning of E_{k15} is equal to the threshold value at which the left tail of the kaon energy spectrum contains 15.83% of the total number of kaons. This measure of separation permits analysis of spectra with the non-Gaussian shape.

For a 2 cm liquid krypton chamber and for incident π- and *k*-mesons with momentum (0.5÷0.8)GeV/c the value of parameter χ, which characterizes the feature of Vavilov distribution [12] varies in the range χ=(0.005÷0.3). It means that the distribution of energy loss has an intermediate shape between Landau (for π-meson) and Gaussian (for *k*-meson at 0.5 GeV/c).

The most precise way to extract the information about the mass of the penetrating particle with the known momentum from multiple measurements of $dE/dx(i)_{mes}$ is to use the maximum likelihood method comparing the measured distribution with the Vavilov distribution. But in this case one should perform complicated computations. A much simpler procedure, which is almost as accurate but uses much less computing time, is the method of the truncated mean [3,13]. This method rejects certain percentage of the lowest and highest of the N measured $dE/dx(i)_{mes}$ values from the calculation of the mean energy loss. The fraction of hits to be rejected is determined by optimizing the resolution. Usually the highest (30÷40)% of the charges are truncated and no truncation is performed at the lower tail of the Vavilov (Landau) distribution.

The resolution of the energy loss measurement, and hence the separation of particles, using the method of the truncated mean depends on the number N_{qg} of samples used. This dependence has been studied by analyzing the mean values of 2 or 3 minimal $dE/dx(i)_{mes}$. Another method was studied, which varies the number of selected values of $dE/dx(i)_{mes}$. The following formula describes the number of lowest values N_{mn} of $dE/dx(i)_{mes}$ taken into calculation of mean value of energy loss dE/dx^* :

$$N_{mn}=N_{qg}-IFIX[k_s(N_{qg}-1)(dE/dx_{max}-dE/dx_{min})/dE/dx_{min}]$$

Ten values of k_s were used in each calculation. Then the optimal value of k_s=1.05 was determined by analyzing the results at the 4 momentum values (Fig 7 a,b,c,d) for N_{gr}=7. For another set of parameters the optimal value of k_s is usually different. The minimal number of quasi gaps taken into account N_{mn} was limited: $N_{mn} \geq 1$.

Fig. 8 a,b depict the distribution of N_{mn} for pion and kaon analysis in the case of the optimal value of k_s. For the momentum range (0.5÷0.8) GeV/c this method of flexible rejection gives better separation of π- and k- mesons than the method of truncated mean.

2.4 Predictions on the particle separation

The results presented here are centered around two ionization chamber geometries: one with 2 cm and the other with 4 cm gap width L of liquid krypton. Drift time was T_{dr}=6.6 μs and 13.2 μs respectively. Another essential parameter K_w which describes the intensity of recombination is the ratio of the collected to primary released numbers of free electrons. The calculations were done mainly for K_w=1.25 (80% collection [4]) and for K_w=3.0 (33%). The latter value corresponds to the case [6] of non-purified Kr. Most of the following results were obtained using the model of a real 10 bit FADC with ±1/4LSB (least significant bit) integral and differential nonlinearity.

Fig. 9 a,b depicts the dependence of separation (POO%) on the momentum of particles for few numbers of quasi-gaps (N_{qg}) when fixed numbers (2 or 3) of lowest $dE/dx(i)_{mes}$ were used for analysis. The POO% for raw amplitude spectra are also plotted for comparison; the curves hereafter are simple power-law fit lines.

When the method of flexible rejection with a varied number of N_{mn} was used the particle separation under the same condition becomes better (Fig. 10a). If non-purified Kr is used, which causes significant loss of collected charge [6], then the calculated selection property of the chamber will degrade drastically (Fig. 10b).

The improvement of selection capability of particle species can be obtained by increasing the thickness of the ionization chamber (increasing N_{mn} at the same noise influence) or by "decreasing" the noise influence. In the ideal case of zero noise level the best particle separation could be achieved using one lowest value of $dE/dx(i)_{mes}$ by increasing the number of quasi-gaps (i.e. decreasing its thickness).

For real noise condition and for increased thickness of the gap L=4 cm the simulated result is demonstrated in Fig. 11a. Calculation for a 6 cm gap (T_{dr}=19.8 μs) gives POO%=9% at momentum 0.8 GeV/c. However no reference measurement of the real preamplifier noise in the range of frequency corresponding to such drift time was done, so the prediction for long signal analysis is not reliable.

The outcome of the Monte Carlo showed no significant degradation of particle separation when models of ideal (10 bit with ideal linearity) and real (10 or 8 bit) FADC with integral and differential nonlinearity equal ± 1/4LSB was used. For the 8 bit model of real FADC with the same ± 1/4LSB nonlinearity the separation capability changes slightly (Fig. 11b), probably because of the particular nonlinearity of FADC. The values of drift time were varied in ±30% range and no significant change in POO% was found either. The "turn off" of ^{85}Kr β-decay does not improve significantly the separation capability (relative improvement of POO% is about 5%).

For the case of a double gap (2*2 cm) reading (when two successive gaps of the flat chambers are read by one preamplifier) the ionization space distributions are superimposed. Fig. 12 depicts degradation of separation at 0.8 GeV/c in comparison with the same 4 cm thickness chamber (Fig. 11a).

3. Conclusion

The described method of the signal shape analysis for rejection of energetic δ-electrons permits particle identification at relatively low momentum. The predicted particle separation power for π- and k-mesons of 0.8 GeV/c momentum in a 4 cm gap of a LKr chamber is about 2σ. At higher momentum the particle separation for the above mentioned geometry does not permit overcoming this level because of low value of RDE_{rst}.

In the case of relatively small free electron life time one should normalize $dE/dx(i)_{mes}$ to correct the systematic decay of the "second derivative". Such normalization involving the cumulative distribution function for particular spectra $dE/dx(i)_{mes}$ obtained in some narrow momentum range showed suitable result.

The experimental measurement with a 2 cm LKr chamber was performed on the beam at CERN. Now data handling is in progress.

Appendix A

Because of non uniform space distribution of the ionization along the track the fast (electron) response of the chamber is not proportional to the energy released in the gap. It is known as "ballistic deficit" [14]. In [4] this kind of distortion of the the energy resolution was called "the geometrical factor". The code permits one to calculate the output signal of an *RC*-2*CR* (*RC*-*CR*) shaper connected to an integrating preamplifier. The relative difference Δ_r of the shaper response U_{sh} and the value U_{q0}, proportional to the charge released in the gap: $\Delta_r=(U_{sh}-U_{q0})/U_{sh}$, was calculated for different momenta and different shaper parameters.

For this calculation the preamplifier noise was "turned off" in order to see the influence of δ-electrons alone. Fig. 13 shows that a decrease in shaping time improves linearity of the response, but the signal also decreases while the noise grows [4]. The rms of these distributions for single- and double-gap chambers and for various values of *RC*-2*CR* shaping time are shown below:

Table 3. Relative nonlinearity of response Δ_r as a function of the shaping time for single (2 cm) and double (2*2 cm) chambers.

τ_{sh} (μs)	0.1	0.3	0.8	2.0	8.0
rms_{single}	4.24	6.77	9.08	10.08	7.92
rms_{double}	3.48	5.65	7.76	8.36	6.56

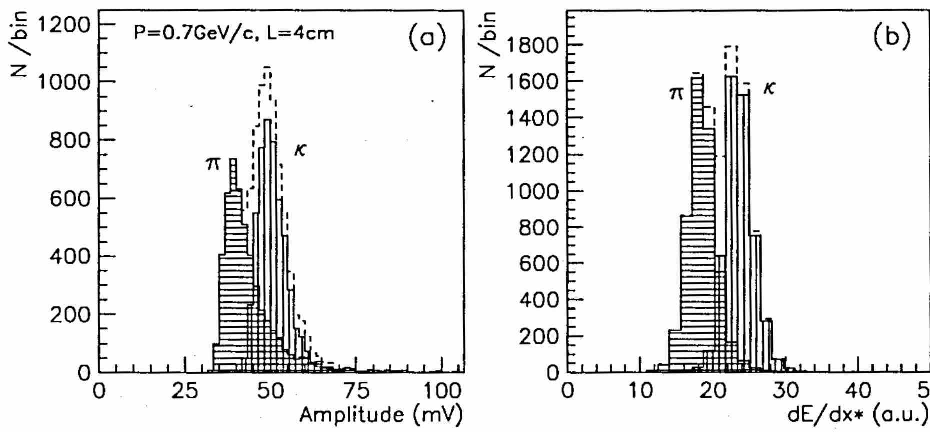

Fig. 1 a) Calculated amplitude spectra for π- and k-mesons (P=0.8 GeV/c) in the 4 cm gap of LKr chamber.
b) dE/dx* spectra after rejection of the energetic δ-electrons.

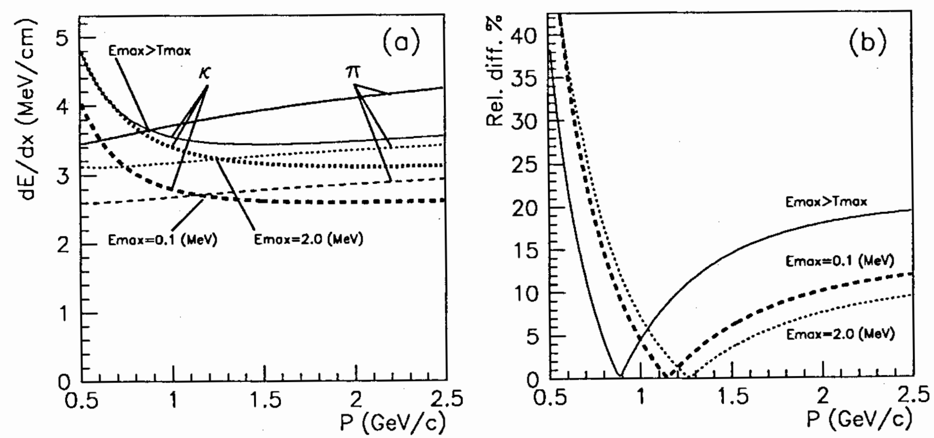

Fig. 2 a) Total ($E_{max}\geq T_{max}$) and restricted (E_{max}= 0.1; 2.0 MeV) energy loss of pions and kaons in LKr.
b) Relative difference of restricted energy loss for pion and kaon.

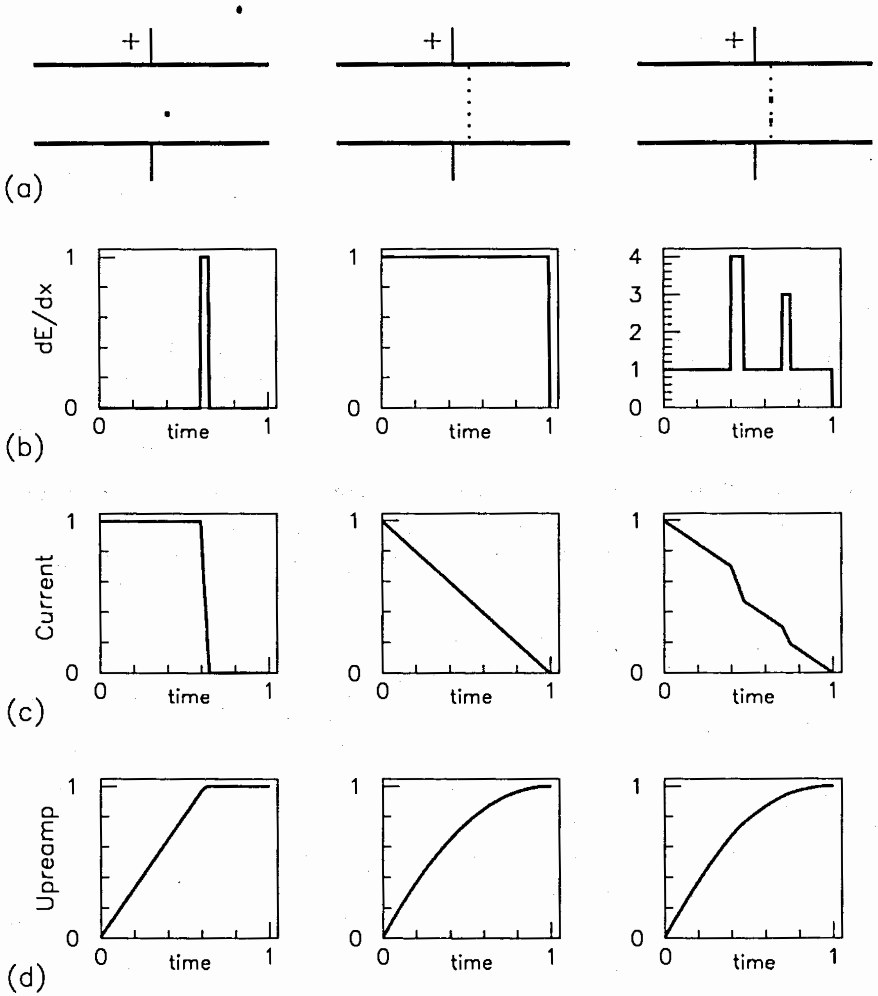

Fig. 3. Fig. 4. Fig. 5.

Fig. 3,4,5 The shapes of current at the input of the integrating preamplifier and output signals for different space distribution of ionization in the gap of the uniform ionization chamber (see text).

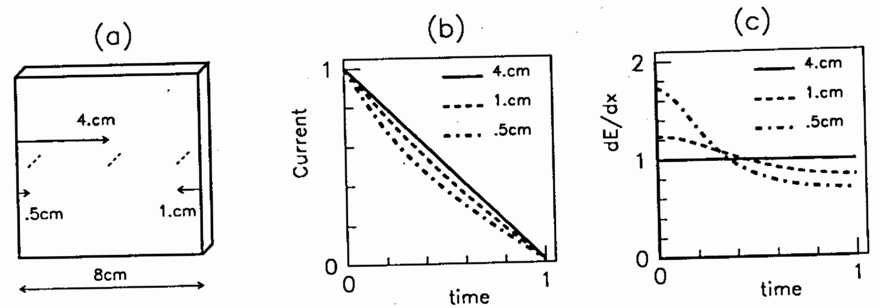

Fig. 6 The dependence of the current shape and its first derivative on the distance to the pad edge for the case of uniform ionization in the infinite flat ionization chamber (see text).

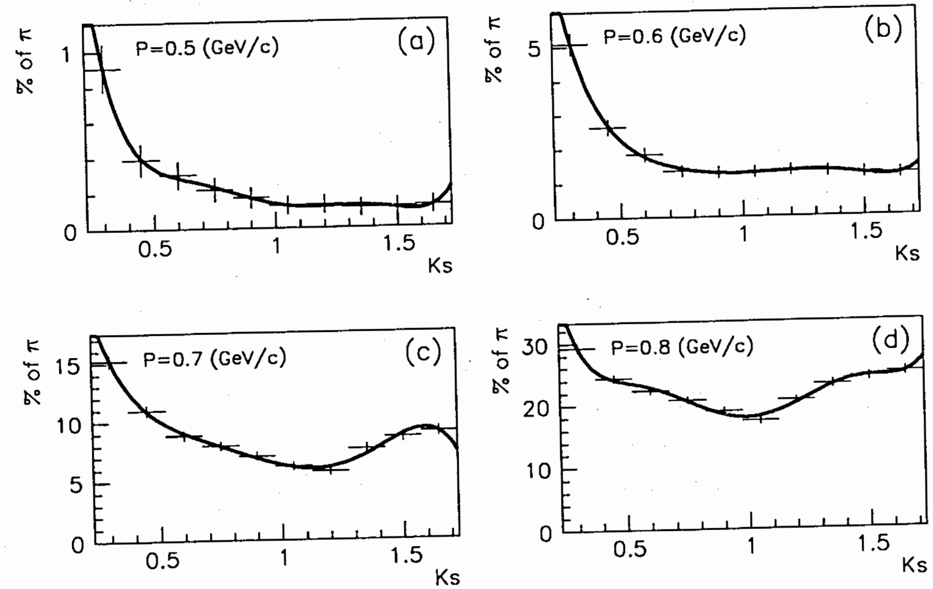

Fig. 7 Calculated particle (π-K) separation (P00%) as a function of k_s for different momenta (see text). L=4 cm, N_{gr}=7.

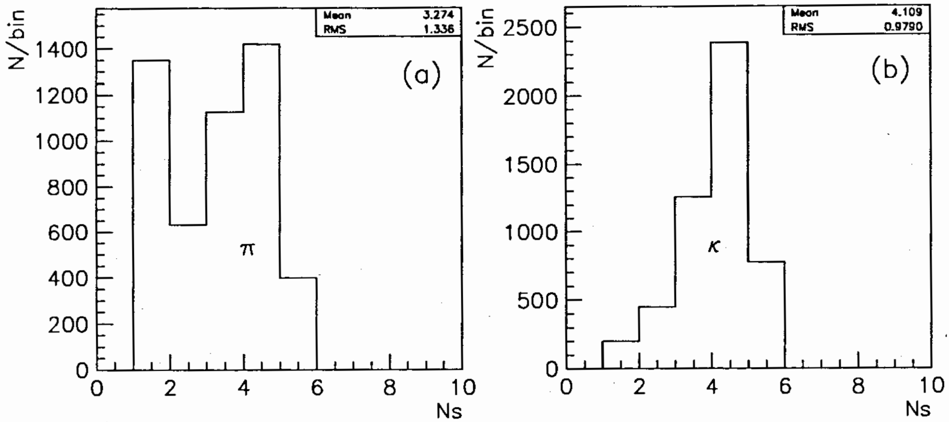

Fig. 8 Numbers of the lowest values of $dE/dx(i)_{mes}$ used in calculation of flexible rejected mean dE/dx^* at the optimum value of k_s for: a) pion; b) kaon analysis. P=0.7 GeV/c, L=4 cm, N_{gr}=7.

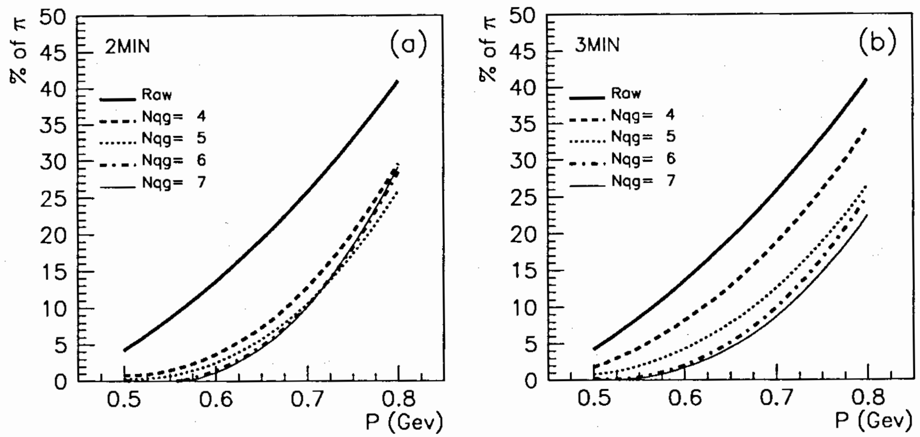

Fig. 9 Calculated particle (π-K) separation (POO%) using 2 (a), or 3 (b) lowest dE/dx(i) mean values. L=4 cm, Tdr=13.2 μs, k_w=1.2, 10bit FADC with ±1/4LSB nonlinearity.

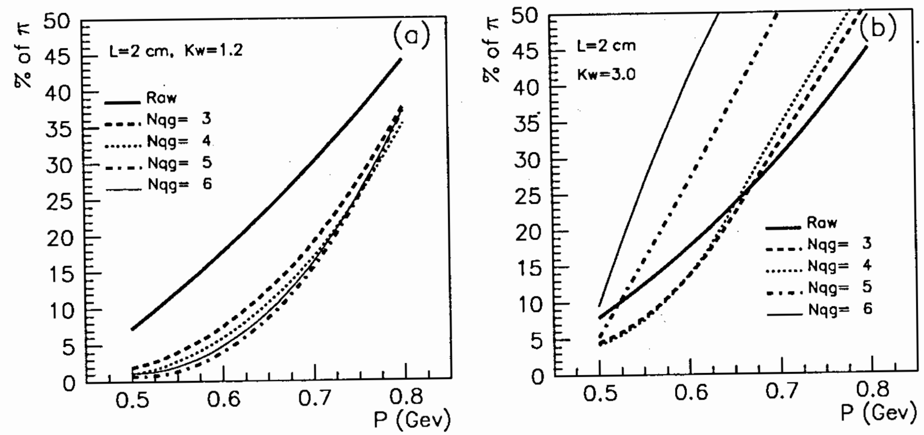

Fig. 10 Optimal particle (π-K) separation (POO%) using method of flexible rejected mean. L=2 cm, Tdr=6.6 μs, 10bit FADC with ±1/4LSB nonlinearity, a) k_w=1.2; b) k_w=3.0 (80% & 30% charge collection).

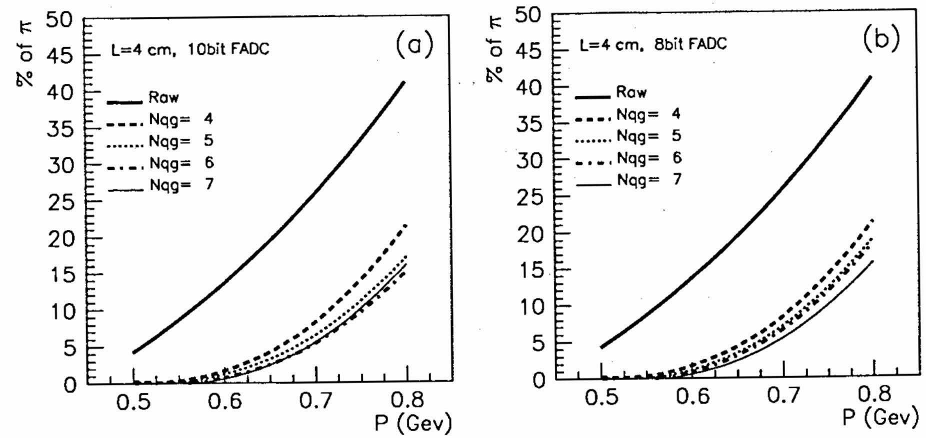

Fig. 11 Optimal particle (π-K) separation (POO%) using method of flexible rejected mean. L=4 cm, Tdr=13.2 μs,
a) 10bit FADC with ±1/4LSB nonlinearity;
b) 8bit FADC with ±1/4LSB nonlinearity.

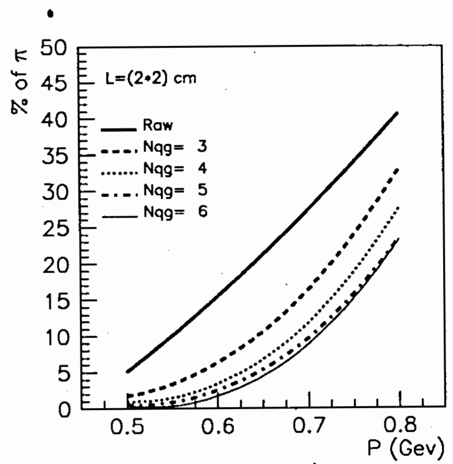

Fig. 12 Optimal particle (π-K) separation (P00%) using method of flexible rejected mean. L=(2*2) cm, Tdr=6.6 μs, k_w=1.2, 10bit FADC with ±1/4LSB nonlinearity (double gap).

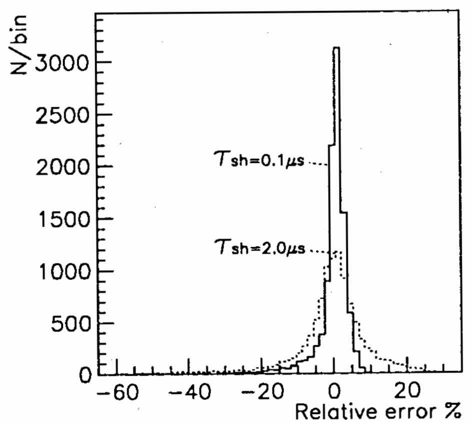

Fig. 13 Spectra of calculated signals in 2 cm Kr for icident π- at P=0.8 GeV/c at the output of RC-2CR shapers (without preamplifier electronic noise influence and ^{85}Kr β-decay).

It is known [4,15] that for MIP the free electron yield reaches the level of (80÷94)% of the charge released in the gap of the ionization chamber. So one can conclude that the effect of the strong recombination near the end of the δe- path does not cause a drastic decrease in nonuniformity of spatial distribution of ionization, and hence does not significantly improve linearity of the response of the read-out method.

Acknowledgements

This work would not have been possible without the contribution and encouragement of Prof. F. Palombo of the University of Milan. I wish to thank Dr. A.I. Kalinin for constructive discussions.

References

[1] T. Doke, NIM A327 (1993) 113.
[2] V.M. Aulchenko et al., NIM A327 (1993) 193.
[3] M. Hauschild et al. NIM A314 (1993) 74.
[4] V.M. Aulchenko et al. NIM A316 (1992) 8.
[5] U. Fano, Ann. Rev. Nucl. Sci. 13, 1 (1963).
[6] E. Aprile et al. NIM A327 (1993) 25.
[7] K-H. Weber NIM 25 (1964) 261.
[8] W.F. Schmidt NIM A327 (1993) 85.
[9] R.M. Sternheimer, R.F. Peierls Phys. Rev. B3 (1971) 3681.
[10] V.M.Aulchenko et al., NIM A289 (1990) 468.
[11] B.Rossi, *High Energy Particles*, Prentice-Hall, Inc., Englewood Cliffs, NJ, 1952.
[12] P.V. Vavilov, Sov. Phys. JETP 32,4 (1957) 922.
[13] D.Jeanne et al. NIM A111 (1973) 287.
[14] J.R. Gigante NIM 111 (1973) 345.
[15] Th. Lindblad et. al. NIM A215 (1983) 183.

Received by Publishing Department
on March 22, 1994.